American Mineralogist, Volume 85, pages 1497–1502, 2000

Cation distribution in synthetic zinc ferrite ($Zn_{0.97}Fe_{2.02}O_4$) from in situ high-temperature neutron powder diffraction

ALESSANDRO PAVESE,[1,2,*] DAVIDE LEVY,[3] AND ANDREAS HOSER[4]

[1]Dipartimento Scienze della Terra-Università degli Studi di Milano, Via Botticelli 23, 20133 Milano, Italy
[2]National Research Council, Centro di Studio per la geodinamica alpina e quaternaria, Via Mangiagalli 34, 20133 Milano, Italy
[3]European Synchrotron Radiation Facility, ESRF-F 38043, Grenoble Cedex, France
[4]Berlin Neutron Scattering Center, BENSC, Hahn Meitner Institut-D 43100 Berlin, Germany

ABSTRACT

Neutron powder diffraction experiments at high temperature (300–1600 K) were performed at BENSC (Berlin, D), on synthetic $Zn_{0.97}Fe_{2.02}O_4$, to investigate the cation partitioning of Zn and Fe over the tetrahedral and octahedral sites as a function of *T*. The data analysis combined Rietveld structure refinements with minimization techniques. The thermodynamic behavior of the thermally activated order-disorder transformation occurring in Zn-ferrite was interpreted by the O'Neill-Navrotsky model ($\alpha = 49.3 \pm 0.4$ and $\beta = -31.6 \pm 2.0$ kJ/mol) and by the equilibrium Landau theory. We obtain $\lambda_2 = 2.813 \pm 0.002$/K, $T_c = 1022 \pm 37$ K using a "pure" Landau approach, and $h = -1.164 \pm 0.002$ kJ/mol, $c = 9.868 \pm 0.06$ kJ/mol, $T_c = -742 \pm 10$ K, if the configurational contribution to entropy is explicitly accounted. The results are in agreement with the earlier powder XRD work of O'Neill (1992) on quenched specimens, but extend the temperature over which measurements were obtained to 1600 K.

INTRODUCTION

Ferrite spinels (space group $Fd\overline{3}m$) have the general chemical composition AFe_2O_4, where A is a divalent cation. Their unit cell contains 32 O atoms in cubic closest-packing, eight tetrahedral (T) and 16 octahedral (M) sites, hosting Fe and A cations. In the ideal "normal" structure the A-cations enter fourfold coordination, whereas iron occupies the M-sites; in the "inverse" structure, common in ferrites, all of the A values move to the octahedral sites, and are replaced in the fourfold-coordination positions by half the Fe atoms. Intermediate configurations often occur, and are described by the inversion parameter *x* (see O'Neill and Navrotsky 1983) which accounts for the amount of Fe on the tetrahedral sites. Ferrites have been studied mostly for their magnetic properties, which depend on the distribution of iron over the two sublattices corresponding to the T- and M-sites.

Zinc ferrite (franklinite) was inferred to have a normal cation distribution regardless of the temperature of preparation or of equilibration, according to Mössbauer spectroscopy [see Marshall and Dollase (1984), and references therein]. Such a notion, however, was at variance with elementary crystal-chemical considerations, and motivated a study by O'Neill (1992), which demonstrated that order disorder reactions occur in this compound as well. O'Neill (1992) performed his investigations on quenched specimens. Now, taking into account that: (1) no in-situ high-temperature investigation on Zn ferrite is available in literature, (2) the results of O'Neill (1992) rely upon quenched samples and do not provide information above 1200 K, we carried out a suite of in-situ high-temperature neutron powder diffraction experiments, on a synthetic sample, to investigate the order-disorder (OD)-reactions occurring in Zn ferrite. Given that zinc and iron have remarkable neutron scattering length contrast [$b_{Zn} = 0.568$ vs. $b_{Fe} = 0.954$ 10^{-12} cm, against $Z_{Zn} = 30$ vs. $Z_{Fe} = 26$; neutron scattering lengths values from General Structure Analysis System (GSAS) (Larson and Von Dreele 1987; Lovesey 1984)], neutron diffraction is an appropriate technique to obtain the Zn and Fe distribution, which was determined, in this work, by combining Rietveld structure refinements with minimization techniques.

EXPERIMENTAL METHODS

Sample

The sample used was synthesised by solid state reaction of oxides, heating for 48 hours at 1400 K a stoichiometric mixture of analytical purity ZnO and Fe_2O_3 reagent grades, compressed into a 10 g pellet to favor their reaction. The temperature was then decreased at ≈15 K/h, down to 800 K, maintained for 24 hours, and finally brought to room temperature at the same rate; the process took about one week. The crystallinity of the sample was checked by X-ray powder diffraction by means of a Bragg-Brentano PHILIPS X'PERT diffractometer, using NBS-silicon as an internal standard. The cell parameter [$a = 8.4418(5)$ Å] determined by full profile fitting method is in agreement with values from the literature for synthetic Zn ferrite (Waerenborgh et al. 1994; O'Neill 1992).

We measured ^{57}Fe Mössbauer spectra at room temperature using a conventional constant acceleration spectrometer (rhodium matrix ^{57}Co source with nominal strength 50 mCi) to investigate the oxidation state of iron. Approximately 20 mg of finely ground material was suspended in vaseline, placed in

---

[*] E-mail: pavese@p8000.terra.unimi.it

0003-004X/00/0010–1497$05.00

a lead container, and wrapped in a plastic foil. The spectrum was fit to a Lorentzian-type profile function, yielding δ(isomer shift) = 0.356(1) mm/s, ΔE_Q(quadrupolar split) = 0.338(2) mm/s, Γ(Lorentzian FWHM) = 0.290(1) mm/s. Mössbauer spectroscopy indicated the occurrence only of Fe^{3+}.

Chemical analyses were performed by air-acetylene flame atomic absorption spectroscopy (2380 Perkin-Elmer Spectrophotometer), with hollow cathode lamps as light sources. Zn (213.9 nm; sensitivity ≈0.018 mg/L) and Fe (248.4 nm; sensitivity ≈0.10 mg/L) metals were used as calibrants. Two solutions with sample concentrations of 0.2079 g and 0.2035 g per 250 mL and 200 mL, respectively, were prepared [mix of 4 mL of HCl (37%) and 2 mL HNO_3 (65%) as solvent], and ten 6-s long absorbance measurements performed for each. By constraining Fe to have a 3+ valence state, we derived the composition $Zn_{0.969(7)}Fe_{2.021(15)}O_4$.

Powder diffraction

A total of fourteen data sets were recorded over the temperature range 300–1600 K at BENSC (Berlin Neutron Scattering Centre), on the E2 powder diffractometer (BENSC User Guide 1996: Neutron scattering instrumentation at the research reactor BER II), using the synthetic sample described above. Figure 1 shows the experimental and calculated patterns at 300 and 1500 K, respectively. The sample was previously powdered by manual grinding, so as to achieve a crystallite size smaller than 20 mm. Approximately 3 cm^3 of sample were loaded into a cylindrical vanadium can, bathed in a neutron flux of 2×10^6 $n/cm^2/s$, and maintained under vacuum (~10^{-6} bar) by a turbomolecular pump. The measurements were performed with $\lambda \approx 1.220$ Å, by a Ge(311) monochromator, with energy bandpass of $\Delta\lambda/\lambda \approx 10^{-3}$. The neutrons scattered were recorded with a 400-channel linear multidetector, covering 2θ = 20–100°; a radial collimator was used as a filter to reduce the parasitic diffraction signals due to the high temperature chamber. The present experimental setup allowed resolution of $\Delta d/d \approx 10^{-3}$, sufficient to refine highly symmetric structures having modest Bragg peak overlaps. High temperature was achieved by means of a resistance furnace, equipped with an ILL-designed controller, which restricts the temperature fluctuations within ±3 K from the set T-value. Every data collection required approximately 4 hours. The data collection time was doubled for the data sets above 1000 K, to compensate for the reduction in intensity of the diffracted signals due to the increased atomic thermal motion. The raw diffraction patterns were corrected for detector efficiency and for conditioning cell absorption by laboratory supplied software.

The structure refinements were made with the GSAS software package (Larson and Von Dreele 1987). The experimental peak diffraction profiles were modelled by Gaussian functions, and the FWHM parameterized as $\sigma^2 = \sigma_0 + \sigma_1\tan(\theta) + \sigma_2\tan(\theta)^2$. The σ_2-coefficient was allowed to vary during the refinements, to account for the structural strain which is sensitive to T, whereas σ_0 and σ_1 were determined from a reference data collection on Si, and from the room temperature pattern on the present sample, respectively. The circular arrangement of the detector caused the experimental patterns to be affected by moderate asymmetry that was accounted for by the Howard (1982) model; the background, practically flat, was modelled using a four-term cosine function series. The cell edge, the coordinate of oxygen, the isotropic atomic displacement parameters, along with the instrumental parameters mentioned above, were allowed to vary during the structure refinements.

To properly account for the slight non-stoichiometry of the sample, the cation partitioning was determined by the method adopted by Pavese et al. (1999a, 1999b). First, the T- and M-site neutron scattering lengths (b_T and b_M, respectively) were refined, upon requiring the conservation of the total neutron scattering length of the cell, calculated according to the nominal composition from the chemical analyses; this was achieved by constraining the shifts of b_T and b_M on the least square cycles (*i.e.*, δb_T and δb_M), to fulfil the relationship beneath

$$\delta b_T = -2\ \delta b_M. \qquad (1)$$

Then, the cation partitioning was obtained by minimizing [MINUIT code, James and Roos (1975)] the following function

$$\Phi = \Sigma_j(A_{obs,j} - A_{calc,j})^2 w_j \qquad (2)$$

where $A_{obs,j}$ are measured quantities (site neutron scattering lengths, chemical composition) or crystal chemical constraints (full site occupancy), and $A_{calc,j}$ are the theoretical counterparts, calculated as a function of the cation-vacancy partitioning; w_j are weights set equal to $1/\sigma_j^2$. The vacancy distribution was fixed by preliminary refinements assuming the stoichiometric composition, i.e., $ZnFe_2O_4$, then re-scaling the occupancy factors of Zn and Fe so as to achieve the experimental chemical composition. The inversion parameter so determined, i.e., the amount of Fe on the tetrahedral sites, is henceforth indicated as x. To assess the uncertainty due to vacancies, whose amount is of the same order of magnitude of the uncertainties upon composition, we also determined the inversion parameter as the average of the values of x obtained imposing the largest and the least concentration of vacancies on the T-sites, compatible with the constraints above. The inversion parameter calculated in this way is addressed as $<x>$.

RESULTS AND DISCUSSION

The structural parameters are in Table 1. The uncertainties on x, or $<x>$, estimated on the basis of the uncertainties upon chemical composition and site neutron scattering lengths, are 0.017, up to 1300 K, 0.02 at 1400 K, and 0.03 at 1500 K. Note that x and $<x>$ are by far within 1s apart; given that the x-values yield thermodynamic parameters affected by systematically smaller uncertainties, we refer in the following to x. Because of the chemical composition of our sample, the lower limit of x is 0.02 and not 0.0 as for a completely stoichiometric spinel. At room temperature Fe is nearly fully ordered into the M-site. This partitioning is somewhat surprising: if the conditions of synthesis are considered and compared with those of the samples of O'Neill (1992) one would expect to observe a more disordered distribution. However, the occurrence of vacancies might speed up re-ordering processes (O'Neill 1997). The Zn-Fe distribution we observed shows negligible variations upon

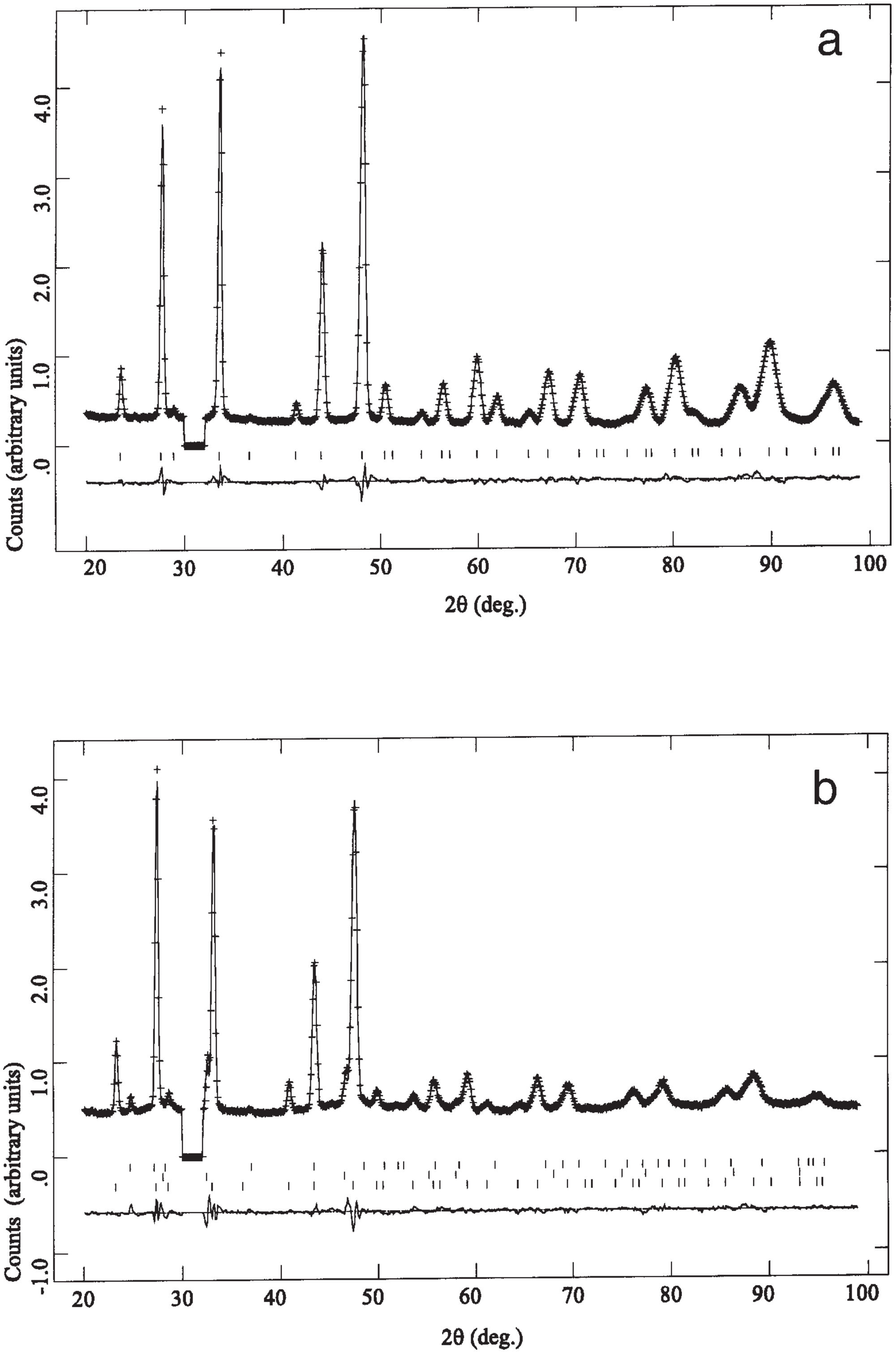

FIGURE 1. Neutron powder diffraction patterns (λ = 1.225 Å) at 300 K (**a**) and at 1500 K (**b**). Experimental and calculated patterns are crosses and solid lines, respectively. In **b**, the positions of the peaks of ZnO, FeO, and spinel are shown as short vertical lines (first, second, and third row, respectively). In **a**, only spinel peak positions are shown. The lowest curve is the residual.

TABLE 1. Refined crystallographic parameters

T (K)	a	u	U_{Ox}	U_M	U_T	b_T	x	$<x>$	wRp
300	8.4418(5)	0.2603(1)	0.80(6)	0.83(6)	0.39(9)	0.5716(30)	0.0240	0.0228	4.7
500	8.4560(5)	0.2602(1)	1.18(6)	1.12(6)	0.78(10)	0.5747(30)	0.0262	0.0285	4.6
700	8.4713(5)	0.2601(1)	1.47(6)	1.41(6)	1.15(10)	0.5737(30)	0.0221	0.0266	4.5
800	8.4785(5)	0.2599(1)	1.69(7)	1.52(6)	1.35(11)	0.5820(30)	0.0419	0.0437	4.3
850	8.4827(5)	0.2597(1)	1.77(7)	1.62(6)	1.39(11)	0.5879(30)	0.0548	0.0588	4.2
900	8.4870(5)	0.2596(1)	2.13(7)	1.52(6)	1.57(11)	0.5921(30)	0.0709	0.0697	4.3
950	8.4914(5)	0.2594(2)	2.26(7)	1.59(6)	1.70(12)	0.5980(30)	0.0778	0.0852	4.3
1000	8.4956(5)	0.2595(2)	2.08(7)	1.92(7)	1.72(12)	0.6040(30)	0.0936	0.1007	4.2
1100	8.5038(5)	0.2592(2)	2.27(7)	2.15(7)	1.84(12)	0.6180(30)	0.1341	0.1369	4.1
1200	8.5130(5)	0.2589(2)	2.59(8)	2.29(8)	2.13(13)	0.6421(30)	0.1975	0.1993	4.3
1300	8.5220(5)	0.2586(2)	2.89(8)	2.50(8)	2.04(13)	0.6481(30)	0.2216	0.2148	4.0
1400	8.5318(5)	0.2585(3)	3.29(1)	2.72(1)	2.11(19)	0.6800(40)	0.3007	0.2976	5.7
1500	8.5450(5)	0.2577(4)	3.57(1)	3.22(1)	2.83(29)	0.6937(50)	0.3403	0.3329	6.1

Notes: a = Lattice parameter (Å); u = oxygen co-ordinate; U = isotropic atomic displacement parameters (Å^2 × 100) of oxygen, T- and M-sites; b_T = T-site neutron scattering length (10^{-12} cm) from Rietveld refinement; x = occupancy factor of Fe at the tetrahedral site; $<x>$ = occupancy factor of Fe at the tetrahedral site determined as the average of the inversion parameter values obtained imposing the least and the largest content of vacancies on the T-sites, compatible with the constraints discussed in the text; $wRp = \mathrm{sqrt}[\Sigma(I_o\text{-}I_c)^{2*}w/\Sigma I_o^{2*}w] \times 100$. The uncertainties on x are reported in the text.

heating up to 800 K (Fig. 2), either due to slow reaction kinetics or due to the equilibrium values of x not being significantly different. At higher temperatures, x smoothly trends up to 1500 K (Fig. 2), but at 1600 K it exhibits an abrupt jump upward (not reported in Figures), ascribed to partial reduction of Fe by oxidation of the vanadium sample can [i.e., $ZnFe_2O_4 + V \rightarrow ZnO + 2\,FeO + VO$], as hinted by the presence of wüstite in the powder diffraction pattern. We therefore ignored data at 1600 K. Reduction of Fe is observed, at much lesser extent, in the powder diffraction pattern at 1500 K. For this reason, we treated the powder diffraction pattern at 1500 K using a multiphase profile refinement to account for the presence of FeO and ZnO phases, whose lattice parameters, isotropic atomic displacement parameters, σ_2-profile breadth coefficients (see above for its definition), and relative phase fractions (S_{FeO} and S_{ZnO}) were refined. S_{FeO} and S_{ZnO} were properly constrained according to the stoichiometry of the reaction above, and varied separately from the parameters of the spinel phase; this proved necessary in order for S_{FeO} and S_{ZnO} to achieve convergence. The contribution of VO to the powder diffraction was negligible because of the very low coherent scattering of V. We attained that FeO and ZnO, in the whole, occur by ≈ 8% in weight, with respect to the parent phase. The refinement of the cation distribution in spinel yields $x = 0.335(30)$, if one neglects the multi-phase treatment, and $x = 0.340(30)$, if one uses it. We chose to adopt the result from the multi-phase treatment, given that it is formally correct accounting for all the phases present, though the values of x issued and above reported are by far within 1σ apart.

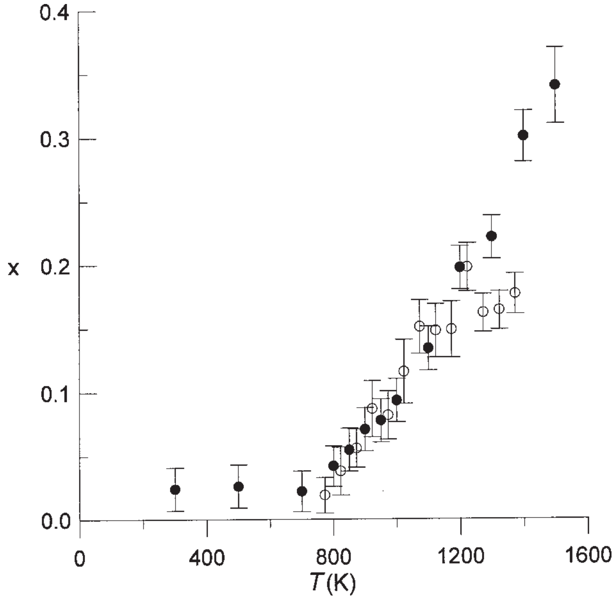

FIGURE 2. The x-inversion parameter as a function of temperature: filled and open circles are the present results and those from O'Neill (1992), respectively.

A comparison with earlier results of O'Neill indicates that: (1) agreement holds up to 1200 K between the two data sets, within ±1σ; (2) above 1200 K, O'Neill's x-curve flattens, "re-ordering being too fast to quench" (O'Neill 1992), whereas the inversion parameter values here obtained increase monotonically; (3) Redfern et al. (1999) state that "the effect of introducing 1 mol% Mg deficiency into the structure" of $MgAl_2O_4$ "is to increase the degree of inversion by $x \approx 0.02$," in their case; such a conclusion is at variance with our observations, if one assumes the results by O'Neill (1992) have been attained from a stoichiometric Zn ferrite. In fact, no systematic shift of the degree of inversion between our results and O'Neill's reveals above 800 K, namely in the thermal region where x has been measured at equilibrium conditions.

O'Neill and Navrotsky (1983, 1984) developed a thermodynamic model, which relates the inversion parameter to the energetics and to the configurational entropy through the following relationship

$$-\mathrm{R}T\ln\left(\frac{x^2}{(1-x)(2-x)}\right) = \alpha + 2\beta\cdot x \qquad (3)$$

where α and β are coefficients to be experimentally determined (see the papers quoted above), and R is the gas constant. We obtain, using x at $T > 750$ K and weights defined as $1/\sigma^2$, $\alpha = 49.3 \pm 0.4$ and $\beta = -31.6 \pm 2.0$ kJ/mol, $\chi^2 = 2.2$ [note that as the uncertainties upon x yield an unrealistically small χ^2 value, we re-scale it by $\Sigma(Y_{obs}-Y_{calc})^2/\Sigma\sigma^2$]. O'Neill (1992) reported $\alpha =$

49.9 ± 2.2 and $\beta = -34.1 \pm 6.9$ kJ/mol; the discrepancy over the absolute values of α and β are 1 and 8%, respectively. The disagreement upon β, though just significant at the ±2s level, might be attributed to the slight compositional differences between our sample and O'Neill's, and to the wider thermal range explored in the present study.

We also tested the O'Neill-Navrotsky model with an additional term aimed at accounting for vibrational entropy contributions, i.e., $-\sigma_e T$. The σ_e is significant just at the $\pm 3\sigma$ level, which hints that the configurational contributions might play a primary role to drive the OD-phenomenology occurring in franklinite.

An alternative approach for the modelling of cation order disorder is provided by the Landau theory, in its form modified to cope with non-convergent cation ordering transformations, which do not cause change of the space group (Carpenter et al. 1994a, 1994b). In this case, the Gibbs energy changes with respect to a disordered configuration can be expressed as

$$G = -\mathrm{h}Q + \frac{1}{2}(T - T_c)aQ^2 + \frac{1}{6}cQ^n \qquad (4)$$

and the equilibrium condition (i.e., $\partial G/\partial Q = 0$) requires fulfilment of the equation

$$\lambda_1(T - T_c)\cdot Q + \lambda_2 Q^{n-1} = 1 \qquad (5)$$

where Q is the order-parameter in the sense of the Landau theory, and it is set equal to $3x/2 + 1$ for spinels (in our case x does not exceed 0.67, and therefore Q is positive); n can be 3, 4, or 6. The dependence on λ_1, λ_2, and T_c, can further be reduced to two parameters [λ_2 and T$_c$, for instance], assuming $Q = Q_0$ at $T = T_0$. One obtains:

$$T = T_c + \frac{(T_c - T_0)}{(1 - \lambda_2 Q_0^{n-1})}\left(\frac{Q_0}{Q}\right)\left[\lambda_2 Q^{n-1} - 1\right]. \qquad (6)$$

We fitted the equation above to our experimental data at $T > 750$ K, using a weighting scheme which accounts for the uncertainties upon temperature and occupancies, and setting $Q_0 = Q_{800}$ at $T = 800$ K. A value of 6 for n provides the best agreement between observed and calculated data. We attained: $\lambda_2 = 2.813(\pm 0.002)$/K and $T_c = 1022(\pm 37)$ K, with $\chi^2 = 1.9$.

The pure Landau model, above discussed, can be enhanced by adding to the Gibbs energy expansion a term $[-T\Delta S(Q)]$ that explicitly accounts for the configurational contribution to entropy, as in the case of the O'Neill-Navrotsky model. The temperature can be expressed as $T(\mathrm{h,c},T_c)$, similarly to the equation above. Such a modified form of the Landau expansion, fitted to our experimental data, yields the following parameters: $h = -1.164 \pm 0.2$ kJ/mol, $T_c = -742 \pm 10$ K, and $c = 9.868 \pm 0.06$ kJ/mol, with $\chi^2 = 1.7$; $a = 0.016$ kJ/mol·K is implied by the boundary condition $Q = Q_{800}$ at $T = 800$ K.

The modified Landau model provides a slightly better agreement with the observed Q values than the pure Landau approach and the O'Neill-Navrotsky expansion (Fig. 3). This likely reflects that the modified Landau approach combines the ability of the pure Landau formalism and of the O'Neill-Navrotsky expansion to model energetic and configurational contributions, respectively. A straightforward calculation proves that the configurational contribution to entropy is approximately 50% larger than the vibrational one.

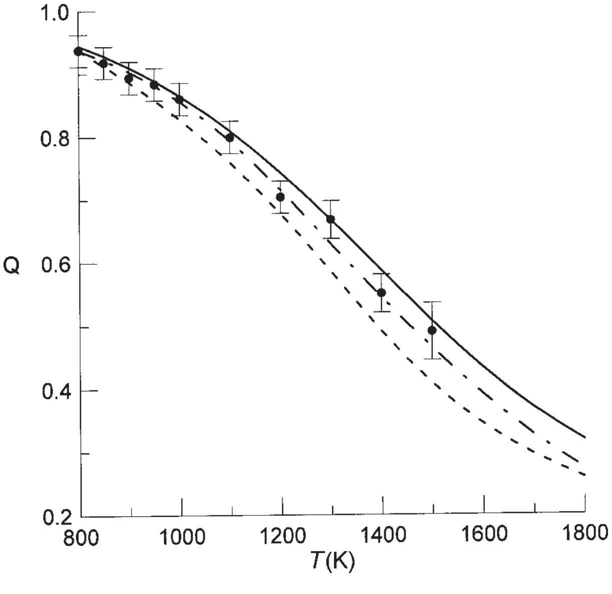

FIGURE 3. Q-order parameter derived according to the O'Neill model (solid line), the pure Landau theory (dashed line), and the modified Landau approach (dot-dashed line); filled circles correspond to the experimental data reported here.

ACKNOWLEDGMENTS

This work was supported by MURST ("Relationships between structure and properties in minerals: analysis and applications" project) and CNR ("Centro di studio per la geodinamica alpina e quaternaria," Milano). Experiments at BENSC were financed by the European Commission through the TMR-LSF Access Programme (contract number CT950060). The authors are grateful to A. Della Giusta and to S.A.T. Redfern for reviewing the manuscript before submission, and to U. Russo, who carried out the Mössbauer measurements here reported.

REFERENCES CITED

Carpenter, M.A., Powell, R., and Salje, E.K.H. (1994a) Thermodynamics of nonconvergent cation ordering in minerals: I. An alternative approach. American Mineralogist, 79, 1053–1067.

Carpenter, M.A. and Salje, E.K.H. (1994b) Thermodynamics of nonconvergent cation ordering in minerals: II. Spinels and orthopyroxene solid solution. American Mineralogist, 79, 1068–1083.

Howard, C.J. (1982) The approximation of asymmetric neutron powder diffraction peaks by sums of Gaussians. Journal of Applied Crystallography, 15, 615–620.

James, F. and Roos, M. (1975) MINUIT-A system for function minimization and analysis of the parameter errors and correlations. Computational Physics Communications, 10, 343–367.

Larson, A.C. and Von Dreele, R.B. (1987) GSAS: General Structure Analysis System. Los Alamos National Laboratory, Report LAUR:86–87.

Lovesey, S.W. (1984) Theory of neutron scattering from condensed matter. Vol. 1. Clarendon Press, Oxford.

Marshall, C.P. and Dollase, W.A. (1984) Cation arrangement in iron-zinc-chromium spinel oxides. American Mineralogist, 69, 928–936.

O'Neill, H.St.C. (1997) Kinetics of the intersite cation exchange in $MgAl_2O_4$ spinel: the influence of nonstoichiometry. In Seventh Annual V.M. Goldschmidt Conference, p. 153. LPI Contribution No. 921, Lunar and Planetary Institute, Houston.

O'Neill, H.St.C. (1992) Temperature dependence of the cation distribution in zinc ferrite ($ZnFe_2O_4$) from XRD structural refinements. European Journal of Mineralogy, 4, 571–580.

O'Neill, H.St.C. and Navrotsky, A. (1984) Cation distribution and thermodynamic properties of binary spinel solid solutions. American Mineralogist, 69, 733–753.

O'Neill, H.St.C. and Navrotsky, A. (1983) Simple spinels: crystallographic parameters, cation radii, lattice energies and cation distribution. American Mineralogist, 68, 181–194.

Pavese, A., Artioli, G., Russo, U., and Hoser, A. (1999a) Cation partitioning versus temperature in $Mg_{0.70}Fe_{0.23}Al_{2.04}O_4$ synthetic spinel, by in situ neutron powder diffraction. Physics and Chemistry of Minerals, 26, 242–250.

Pavese, A., Artioli, G., and Hull, S. (1999b) Cation partitioning versus pressure in $Mg_{0.97}Al_{1.97}O_4$ synthetic spinel, by in situ neutron powder diffraction, American Mineralogist, 84, 905–912.

Redfern A.T., Harrison, R.J., O'Neill H.St.C., and Wood, D.R.R. (1999) Thermodynamics and kinetics of cation ordering in $MgAl_2O_4$ spinel up to 1600°C from in situ neutron diffraction. American Mineralogist, 84, 299–310.

Waerenborgh, J.C., Figureido, M.O., Cabral, M.P., and Pereira L.C.J. (1994) Temperature and composition of the cation distribution in synthetic $ZnFe_yAl_{2-y}O_4$ ($0 \leq y \leq 1$) spinels. Journal of Solid State Chemistry, 111, 300–309.

MANUSCRIPT RECEIVED JANUARY 27, 2000
MANUSCRIPT ACCEPTED JUNE 20, 2000
PAPER HANDLED BY BRYAN CHAKOUMAKOS